

# Ferrocene-based multichannel molecular chemosensors with high selectivity and sensitivity for Pb(II) and Hg(II) metal cations†

María Alfonso, Alberto Tárraga\* and Pedro Molina\*

Received 10th May 2010, Accepted 30th June 2010

DOI: 10.1039/c0dt00450b

The synthesis, electrochemical, optical and cation-sensing properties of ferrocene-imidazoquinoxaline dyads **6**, are presented. Dyad **6a** behaves as a highly selective redox, chromogenic and fluorescent chemosensor molecule for Pb<sup>2+</sup> cations in CH<sub>3</sub>CN solutions; the oxidation redox peak is anodically shifted ( $\Delta E_{1/2} = 110$  mV); in the absorption spectrum a new low-energy band appeared at  $\lambda = 463$  nm, and the emission band is red-shifted ( $\Delta\lambda = 31$  nm) along with an important chelation-enhanced fluorescence factor (CHEF = 276), upon complexation with this metal cation. The dyad **6b**, bearing two additional pyridine rings as substituents, has shown its ability for sensing Hg<sup>2+</sup> cations through three different channels: the oxidation peak is anodically higher shifted ( $\Delta E_{1/2} = 300$  mV), a new low-energy band appears in the absorption spectrum at  $\lambda = 483$  nm, and the emission band was also red-shifted ( $\Delta\lambda = 28$  nm) and underwent an important chelation-enhanced fluorescent factor (CHEF = 227). The changes in their absorption spectra are accompanied by color changes from yellow to orange which allow their potential use for the “naked eye” detection of these metal cations. Linear sweep voltammetry revealed that Cu<sup>2+</sup> cations induced oxidation of the ferrocene unit in both dyads, which is accompanied by an important increase of the emission band.

## Introduction

The development of selective and sensitive imaging tools capable of monitoring heavy- and transition-metal ions has attracted considerable attention because of the wide use of these metal ions and their subsequent impact on the environment and nature.<sup>1</sup> The Hg<sup>2+</sup> ion is considered a highly toxic element, and its contamination is a global problem and a major source of human exposure stems from a variety of natural and anthropogenic sources<sup>2</sup> including oceanic and volcanic emission,<sup>3</sup> gold mining,<sup>4</sup> solid waste incineration, and combustion of fossil fuel.<sup>5</sup> The exposure of mercury even at low concentration leads to digestive, kidney, and specially neurological diseases.<sup>6</sup> Although the pollutant character of mercury has mainly been focused on the occurrence of methylmercury in the marine food chain, the mercury problem is not limited to the aquatic food chain since rice has recently been proposed as the major source for methylmercury intake from food in parts of the Chinese population, and the results indicate that this derivative is more prominent in the rice grains than would be expected from the occurrence of methylmercury *versus* inorganic mercury in the soil.<sup>7</sup> Keeping in view the roles placed by mercury in day to day life, the development of techniques for mercury hazard assessment and mercury pollution management has drawn worldwide attention.<sup>8</sup> Therefore, many laboratories have focused on “colorimetric”,<sup>9</sup> redox active<sup>10</sup> and/or fluorescent<sup>11</sup> highly selective mercury-responsive small-molecule chemosensors.

Among heavy metal, lead is the most abundant and ranks second in the list of toxic substances and is often encountered due to its wide distribution in the environment as well as its current and previous use in batteries, gasoline and pigments. Lead pollution is an ongoing danger to the human health, particularly in children (memory loss, irritability, anaemia, muscle paralysis, and mental retardation),<sup>12</sup> and the environment, as most of the 300 million tons of this heavy metal mined to date are still circulating in soil and groundwater.<sup>13</sup> Despite efforts to reduce global emissions, lead poisoning remains the worlds most common environmentally caused disease.<sup>14</sup> Thus, the level of this detrimental ion, which is present in tap water as a result of dissolution from household plumbing systems, is the object of several official norms. The World Health Organisation established in 1996 guidelines for drinking-water quality,<sup>15</sup> which included a lead maximal value of 10  $\mu\text{g L}^{-1}$ . The US Center for Disease Control (CDC) set standards stating that a 10–19  $\mu\text{g dL}^{-1}$  level of lead in blood poses a potential threat and that diagnostic testing is recommended.<sup>16</sup> Thus, keeping in view the role of Pb<sup>2+</sup>, the detection and monitoring of this metal cation by methods which allow the development of selective and sensitive assays becomes very important. As many heavy metals are known as fluorescence quenchers *via* enhanced spin-orbital coupling,<sup>17</sup> energy or electron transfer,<sup>18</sup> development of fluorescent sensors for Pb<sup>2+</sup> presents a challenge. In this context, considerable efforts have been undertaken to develop fluorescent chemosensors for Pb<sup>2+</sup> ions based on peptide,<sup>19</sup> protein,<sup>20</sup> DNAzyme,<sup>21</sup> polymer,<sup>22</sup> and small-molecule<sup>23</sup> scaffolds. There is, however, a paucity of use of multichannel receptors as potential guest reporters *via* multiple signalling patterns. Specifically, as we report here, the development of multichannel (chromogenic/fluorogenic/electrochemical) Pb<sup>2+</sup> selective chemosensors is, as far as we know, an unexplored subject,<sup>24</sup> and only a few dual chromogenic and redox receptors have been recently described.<sup>25</sup>

Departamento de Química Orgánica, Universidad de Murcia, Campus de Espinardo, 30100, Murcia, Spain. E-mail: pmolina@um.es, atarraga@um.es; Fax: +34 968 364 149; Tel: +34 968 367 496

† Electronic supplementary information (ESI) available: NMR spectra of the new compounds reported. LSV, CV and OSWV, UV-vis and fluorescence titration data. Reversibility experiments, semi-logarithmic plot for determining the detecting limits; <sup>1</sup>H NMR titration data; ESI mass spectra of the complexes formed. See DOI: 10.1039/c0dt00450b

On the other hand, quinoxalines<sup>26</sup> are a well known class of fluorescent compounds with high quantum yields and have attracted much attention due to their potential for speciality and high-technology applications. Recently, a new class of fluorescent anion sensor bearing extended conjugated quinoxalines has been described, which incorporate one or several pyrrolyl units as the anion recognition element.<sup>27</sup> Recently, a new chemosensor molecule based on a ferrocene-azaquinoxaline dyad has been reported, which effectively recognizes  $\text{Hg}^{2+}$  in aqueous environment.<sup>28</sup>

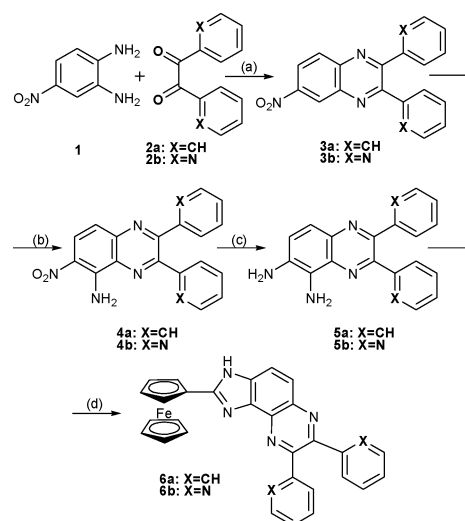
In the context of this work, it has been found that annulation of an additional azaheterocycle, such as an imidazole ring, could impart an interesting behaviour. In this new structural motif, one of the nitrogen atoms of the added heterocyclic system cooperates with the basic nitrogen atom of the quinoxaline ring and consequently enhances the binding affinity towards metal cations. It is expected that the binding ability of the resulting fused imidazo-quinoxaline ring system could be improved if additional binding sites in the guise of azaheterocycles are placed at appropriate positions in the quinoxaline core. On the other hand, in ferrocene derivatives, cation (anion) binding at an adjacent receptor site induces a positive (negative) shift in the redox potential of the ferrocene/ferrocenium redox couple, and the complexation ability of the ligand can be switched on and off by varying the applied electrochemical potential. The magnitude of the electrochemical shift ( $\Delta E_{1/2}$ ) upon complexation represents a quantitative measure of the perturbation of the redox center induced by complexation to the receptor unit.<sup>28b,29</sup>

## Results and discussion

The target receptors **6** were prepared by the following four-step sequence: (a) condensation of the commercially available 4-nitro-*o*-phenylenediamine with the corresponding 1,2-dicarbonyl compound **2** to give quinoxalines **3** (70–89%); (b) amination at position 6 of the quinoxaline ring with 4-amino-1,2,4-triazole in the presence of  $\text{K}^t\text{BuO}$  in DMSO at room temperature to provide **4** (71–90%); (c) reduction of the nitro group with hydrazine in the presence of Pd on charcoal to afford **5** (74–93%), and (d) imidazole-ring formation by reaction of diamines **5** with ferrocenecarboxaldehyde in nitrobenzene at 60–70° to yield **6** (43–48%) (Scheme 1).

Metal recognition properties of these receptors were evaluated by electrochemical, (CV, LSV and OSWV) as well as through spectrophotometric and  $^1\text{H}$  NMR techniques. The titration experiments were further analyzed using the computer programme Specfit.<sup>30</sup>

At first, their electrochemical behaviour was investigated in the presence of several metal cations such as  $\text{Li}^+$ ,  $\text{Na}^+$ ,  $\text{K}^+$ ,  $\text{Ca}^{2+}$ ,  $\text{Mg}^{2+}$ ,  $\text{Cu}^{2+}$ ,  $\text{Zn}^{2+}$ ,  $\text{Cd}^{2+}$ ,  $\text{Hg}^{2+}$ ,  $\text{Ni}^{2+}$  and  $\text{Pb}^{2+}$  as their appropriate salts.<sup>31</sup> Each free receptor exhibited a reversible one-electron redox wave<sup>32</sup> typical of a ferrocene derivative, at the halfwave potential value of  $E_{1/2} = 450$  mV for **6a** and  $E_{1/2} = 530$  mV for **6b**, calculated versus decamethylferrocene (DMFc) redox couple. Titration studies by addition of the above-mentioned set of metal cations to an electrochemical solution of receptor **6a** ( $c = 10^{-3}$  M) in  $\text{CH}_3\text{CN}$  containing TBAP (0.1 M) as supporting electrolyte, demonstrate that while addition of  $\text{Zn}^{2+}$  ( $\Delta E_{1/2} = 60$  mV),  $\text{Cd}^{2+}$  ( $\Delta E_{1/2} = 90$  mV),  $\text{Hg}^{2+}$  ( $\Delta E_{1/2} = 160$  mV), and



**Scheme 1** Synthesis of ligands **6a** and **6b**. Reagents and conditions: (a) acetonitrile, 50 °C; (b) 4-amino-1,2,4-triazole,  $\text{K}^t\text{BuO}$ , DMSO, 30 °C; (c)  $\text{N}_2\text{H}_4 \cdot \text{ClH}$ , Pd/C, reflux; (d) ferrocenecarboxaldehyde,  $\text{PhNO}_2$ , 60–70 °C.

$\text{Pb}^{2+}$  ( $\Delta E_{1/2} = 110$  mV), promotes remarkable responses (Fig. 1 and ESI†), addition of  $\text{Li}^+$ ,  $\text{Na}^+$ ,  $\text{K}^+$ ,  $\text{Ca}^{2+}$ ,  $\text{Mg}^{2+}$ , and  $\text{Ni}^{2+}$  metal ions have no effect on either the LSV or on the CV or OSWV of this receptor, even when present in a large excess. The positive potential shift observed for the  $\text{Fe(II)/Fe(III)}$  redox couple upon complexation by these metal cations can be due to electrostatic repulsion effect between the bound metal cation and the electrogenerated positive charge on the oxidized ferrocenyl subunit. This leads to a decrease of the association constant with the oxidized ligand and to a destabilization of the complex. Thus, the  $\Delta E_{1/2}$  reflects the balance of the interaction of the metal cation between the neutral and the oxidized charged ligand.

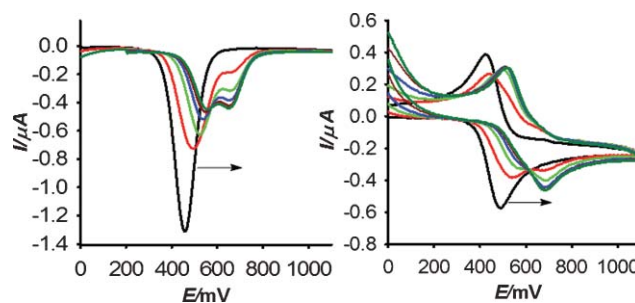


**Fig. 1** Evolution of the OSWV (left) and CV (right) of **6a** ( $10^{-3}$  M) in  $\text{CH}_3\text{CN}$  using  $[(n\text{-Bu})_4\text{N}]\text{ClO}_4$  as supporting electrolyte when  $\text{Pb}(\text{ClO}_4)_2$  is added: from 0 (black) to 1 equivalent (deep green).

Remarkably, LSV studies carried out upon addition of  $\text{Cu}^{2+}$  to the  $\text{CH}_3\text{CN}$  solution of this receptor showed a significant shift of the sigmoidal voltammetric wave towards cathodic current, indicating that this metal cation promote the oxidation of the free receptor (see ESI†).

Similar studies developed using receptor **6b** ( $\text{X} = \text{N}$ ), under the same electrochemical conditions, demonstrate that while addition of  $\text{Zn}^{2+}$  ( $\Delta E_{1/2} = 90$  mV),  $\text{Cd}^{2+}$  ( $\Delta E_{1/2} = 100$  mV),  $\text{Ni}^{2+}$  ( $\Delta E_{1/2} = 80$  mV) and  $\text{Pb}^{2+}$  ( $\Delta E_{1/2} = 70$  mV), promotes a moderate shift of the oxidation wave of the  $\text{Fe(II)/Fe(III)}$  redox couple (see ESI†), addition of  $\text{Hg}^{2+}$  ( $\Delta E_{1/2} = 300$  mV), induced a remarkable shift

**Table 1** Characteristic electrochemical, UV-vis and fluorescent data of the free ligands **6a** and **6b** and their metal complexes

Compound	$E_{1/2}^a$ ( $\Delta E_{1/2}$ )	UV-vis $\lambda_{\max}$ ( $10^{-3}\epsilon$ ) <sup>b</sup>	IP <sup>c</sup>	Fluorescence $\lambda_{\text{emis}}$	$\Phi^d$ (CHEF) <sup>e</sup>	$K_{\text{as}}$	$D_{\text{lim}}^f$
<b>6a</b>	450	270 (3.158), 313 (3.655)		484	$3.6 \times 10^{-4}$		
<b>[6a·Pb<sup>2+</sup>]</b>	560 (110)	253 (2.921), 313 (3.667), 350 (1.696), 463 (0.221)	264, 324, 391, 436	515	0.022 (276)	$8.29 \times 10^5$ ( $\pm 1.39$ ) <sup>g</sup>	$5.25 \times 10^{-6}$
<b>[6a·Zn<sup>2+</sup>]</b>	510 (60)	270 (2.588), 313 (3.645), 350 (1.517), 463 (0.187)	230, 264, 337, 391, 441	—	—	$2.34 \times 10^{11}$ ( $\pm 11.41$ )	$1.31 \times 10^{-5}$
<b>[6a·Cd<sup>2+</sup>]</b>	540 (90)	270 (2.396), 313 (3.236), 350 (1.518), 463 (0.178)	234, 346, 391, 256	—	—	$1.56 \times 10^{11}$ <sup>h</sup> ( $\pm 11.27$ )	$1.72 \times 10^{-5}$
<b>[6a·Hg<sup>2+</sup>]</b>	610 (160)	258 (2.461), 313 (3.079), 350 (1.526), 463 (0.207)	234, 262, 343, 389, 439	—	—	$2.19 \times 10^{11}$ <sup>h</sup> ( $\pm 10.05$ )	$1.15 \times 10^{-5}$
<b>6b</b>	530	277 (2.156), 306 (2.309)		507	$6.1 \times 10^{-4}$		
<b>[6b·Pb<sup>2+</sup>]</b>	640 (70)	284 (1.575), 311 (1.518), 365 (0.881), 483 (0.109)	262, 340	—	—	$1.16 \times 10^{12}$ <sup>h</sup> ( $\pm 11.06$ )	$7.58 \times 10^{-6}$
<b>[6b·Zn<sup>2+</sup>]</b>	590 (90)	284 (1.695), 310 (1.509), 365 (0.776), 483 (0.106)	260, 346	—	—	$9.57 \times 10^{11}$ <sup>h</sup> ( $\pm 12.54$ )	$1.16 \times 10^{-5}$
<b>[6b·Cd<sup>2+</sup>]</b>	620 (100)	284 (2.045), 311 (2.045), 365 (0.888), 483 (0.109)	261, 337, 420	—	—	$5.57 \times 10^{12}$ <sup>h</sup> ( $\pm 18.25$ )	$1.50 \times 10^{-5}$
<b>[6b·Hg<sup>2+</sup>]</b>	830 (300)	284 (1.835), 310 (1.674), 365 (0.701), 483 (0.121)	262, 357, 411	535	0.019 (227)	$1.07 \times 10^6$ <sup>g</sup> ( $\pm 1.93$ )	$1.81 \times 10^{-6}$
<b>[6b·Ni<sup>2+</sup>]</b>	620 (80)	284 (1.870), 311 (1.500), 365 (0.907), 483 (0.105)	263, 339	—	—	$6.61 \times 10^{11}$ <sup>h</sup> ( $\pm 14.26$ )	$9.74 \times 10^{-6}$

<sup>a</sup> mV vs. DMFc. <sup>b</sup>  $\lambda_{\max}$  in nm,  $\epsilon$  in  $\text{dm}^3 \text{mol}^{-1} \text{cm}^{-1}$ . <sup>c</sup> Isosbestic points in nm. <sup>d</sup> Defined as in ref. 36. <sup>e</sup> Defined as in ref. 37. <sup>f</sup> Detection limits in M. <sup>g</sup> In  $\text{M}^{-1}$ . <sup>h</sup> In  $\text{M}^{-2}$ .

of the oxidation potential (Table 1). The results obtained on the stepwise addition of substoichiometric amounts of  $\text{Hg}^{2+}$  metal cation to receptor **6b** revealed a typical two wave behaviour (Fig. 2), which is characteristic of a large equilibrium constant for the binding of this cation by the neutral receptor.<sup>33</sup>

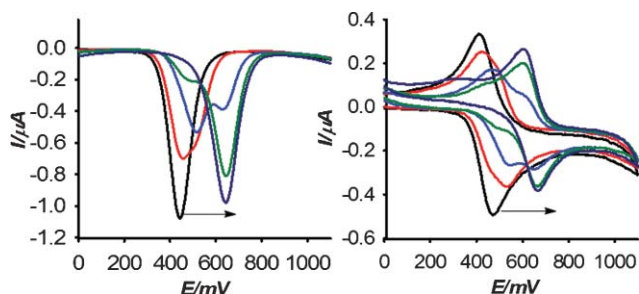


**Fig. 2** Evolution of the OSWV (left) and CV (right) of **6b** ( $10^{-3}$  M) in  $\text{CH}_3\text{CN}$  using  $[(n\text{-Bu})_4\text{N}]\text{ClO}_4$  as supporting electrolyte when  $\text{Hg}(\text{OTf})_2$  is added: from 0 (black) to 1 equivalent (deep blue).

Remarkably, LSV studies carried out upon addition of  $\text{Cu}^{2+}$  to the  $\text{CH}_3\text{CN}$  solution of this receptor showed not only a significant shift of the sigmoidal voltammetric wave towards cathodic currents, indicating that the metal cations promotes the oxidation of the free receptor, but also a gradual shift towards more positive potentials, which is in agreement with a complexation process of the oxidized ferrocenium receptor with  $\text{Cu}^{2+}$  metal cation (see ESI†). A similar behaviour has been observed in ferrocene derivatives bearing pyridine rings as binding site in the presence of  $\text{Cu}^{2+}$  metal cations.<sup>34</sup>

Titration studies by addition of  $\text{F}^-$ ,  $\text{Cl}^-$ ,  $\text{Br}^-$ ,  $\text{AcO}^-$ ,  $\text{NO}_3^-$ ,  $\text{HSO}_4^-$ ,  $\text{H}_2\text{PO}_4^-$ , and  $\text{HP}_2\text{O}_7^{3-}$  anions, as their tetrabutylammonium salts, have also been carried out. These studies demonstrate that while addition of  $\text{F}^-$  and  $\text{HP}_2\text{O}_7^{3-}$  anions induced a clear electrochemical response of these receptors, the addition of  $\text{Cl}^-$ ,

$\text{Br}^-$ ,  $\text{AcO}^-$ ,  $\text{NO}_3^-$ ,  $\text{HSO}_4^-$ ,  $\text{H}_2\text{PO}_4^-$  anionic species had no effect on their CV and OSWV, even when present in a large excess. Thus, the stepwise addition of  $\text{F}^-$  to receptors **6** promotes a clear cathodic shift of the corresponding oxidation waves ( $\Delta E_{1/2} = -300$  mV for **6a** and  $\Delta E_{1/2} = -270$  mV for **6b**) (see ESI†). A way to reveal the formation of hydrogen-bonded complexes under conditions of electrochemical titration is to suppress deprotonation by adding a small amount of acetic acid.<sup>35</sup> Thus, when titration with  $\text{F}^-$  was performed in the presence of  $\text{AcOH}$  (20 equivalents), no electrochemical responses were noticed. On the one hand, upon titration with a strong base, such as  $\text{Bu}_4\text{NOH}$ , the same cathodic shift of the receptor's oxidation wave was observed. These results revealed that, in both cases the addition of  $\text{F}^-$  leads to deprotonation of the neutral receptors.

Interestingly, the stepwise addition of  $\text{HP}_2\text{O}_7^{3-}$  to receptor **6a** induced the progressive appearance of two new oxidation waves, cathodically shifted by  $\Delta E_{1/2} = -80$  mV and  $\Delta E_{1/2} = -300$  mV, which are associated to a recognition and a deprotonation process, respectively. The intensity of these waves is directly related to the number of equivalents of anion added. Thus, after addition of 0.4 equivalents the intensity of the wave associated to the recognition event, appearing at 370 mV, is higher than that of the wave at 160 mV, due to the deprotonation of the free ligand. However the situation is completely reversed when 2 equivalents of  $\text{HP}_2\text{O}_7^{3-}$  were added (Fig. 3(a)). Under the same conditions, addition of  $\text{HP}_2\text{O}_7^{3-}$  induced a cathodic shift of  $\Delta E_{1/2} = -90$  mV in the oxidation wave of receptor **6b** (Fig. 3(b)) However, when the addition of  $\text{HP}_2\text{O}_7^{3-}$  anion to receptors **6a** and **6b** were performed in the presence of  $\text{AcOH}$  only an oxidation wave, cathodically shifted by  $\Delta E_{1/2} = -80$  mV for **6a** and  $\Delta E_{1/2} = -90$  mV for **6b**, was observed. These results clearly indicate that in the absence of an acidic medium both a deprotonation and a recognition process are taking place simultaneously, while in the presence of a small amount of acetic acid only the corresponding hydrogen-bonded adducts are formed.

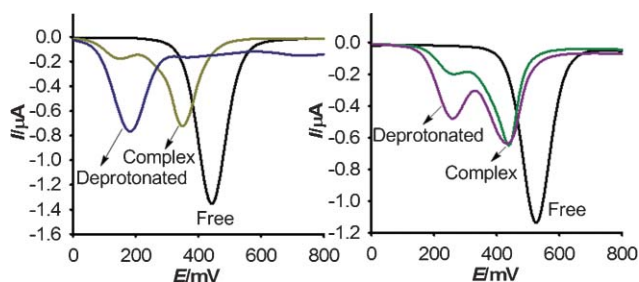


**Fig. 3** OSV of **6a** (left) and **6b** (right) (1 mM) in  $\text{CH}_3\text{CN}/[(n\text{-Bu})_4]\text{ClO}_4$  scanned at  $0.1 \text{ V s}^{-1}$  and in the present of 0.4 equivalents of  $\text{HP}_2\text{O}_7^{3-}$  (deep yellow) and 2 equivalents of  $\text{HP}_2\text{O}_7^{3-}$  (deep blue) (left) and in the present of 0.8 equivalents of  $\text{HP}_2\text{O}_7^{3-}$  (deep green) and 2 equivalents of  $\text{HP}_2\text{O}_7^{3-}$  (deep pink) (right).

Recognition properties of receptors **6** towards metal cations were also evaluated by UV-vis spectroscopy. Titration experiments for  $\text{CH}_3\text{CN}$  solutions of these ligands ( $c = 1 \times 10^{-4} \text{ M}$ ) and the corresponding cations were performed and analyzed quantitatively. It is worth mentioning that no changes were observed in the UV-vis spectrum of **6a** upon addition of  $\text{Li}^+$ ,  $\text{Na}^+$ ,  $\text{K}^+$ ,  $\text{Ca}^{2+}$ ,  $\text{Mg}^{2+}$ ,  $\text{Cu}^{2+}$  and  $\text{Ni}^{2+}$  metal ions, even in a large excess; however, significant modifications were observed upon addition of  $\text{Zn}^{2+}$ ,  $\text{Cd}^{2+}$ ,  $\text{Hg}^{2+}$ , and  $\text{Pb}^{2+}$  (Table 1). In all cases, the addition of increasing amounts of these cations to a solution of **6a** caused a progressive appearance of two weak low-energy bands at  $\lambda = 350$  and  $463 \text{ nm}$  respectively, as well as a decrease of the initial high-energy bands intensities. Well-defined isosbestic points indicate that a neat interconversion between the uncomplexed and complexed species occurs (Table 1). Binding assays using the method of continuous variations (Job's plot) suggest a 1 : 1 (cation/receptor) binding model for  $\text{Pb}^{2+}$  (Fig. 4(b)) and 1 : 2 for  $\text{Zn}^{2+}$ ,  $\text{Cd}^{2+}$ , and  $\text{Hg}^{2+}$  cations (see ESI<sup>†</sup>).

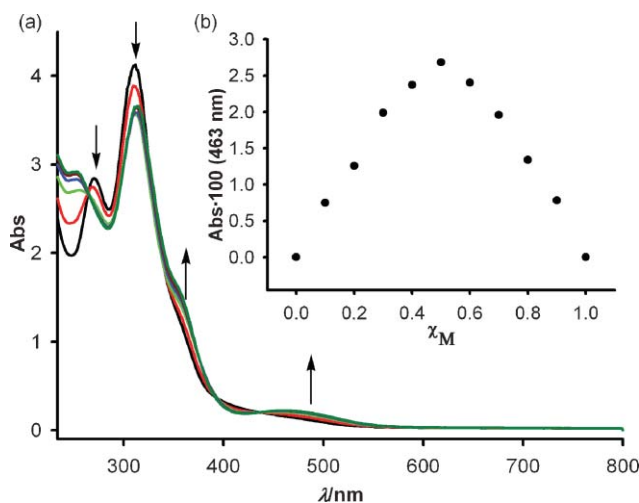


**Fig. 4** (a) Changes in the absorption spectra of **6a** (black) ( $10^{-4} \text{ M}$ ) in  $\text{CH}_3\text{CN}$  upon addition of increasing amounts of  $\text{Pb}^{2+}$  metal cation, until 1 equivalent was added (deep green); (b) Job's plot for **6a** and  $\text{Pb}^{2+}$ , indicating the formation of 1 : 1 complexes. The total  $[\mathbf{6a}] + [\text{Pb}^{2+}] = 10^{-4} \text{ M}$ .

Likewise, addition of these metal cations to a solution of **6b** produces the same perturbations on its absorption spectra: a new low-energy band at  $\lambda = 365 \text{ nm}$  and  $\lambda = 483 \text{ nm}$  appears, with concomitant decreasing of the initial high-energy bands at  $\lambda =$

$227 \text{ nm}$  ( $\epsilon = 2156 \text{ M}^{-1} \text{ cm}^{-1}$ ) and  $\lambda = 306 \text{ nm}$  ( $\epsilon = 2310 \text{ M}^{-1} \text{ cm}^{-1}$ ) respectively (Table 1). These changes occur at approximately three well-defined isosbestic points, at any receptor/cation ratio, suggesting that only one spectral distinct complex was present (Fig. 5 and ESI<sup>†</sup>). In these cases, 1 : 1 binding models were observed for  $\text{Hg}^{2+}$  while 1 : 2 were found for  $\text{Cd}^{2+}$ ,  $\text{Ni}^{2+}$ ,  $\text{Zn}^{2+}$  and  $\text{Pb}^{2+}$  metal cations.

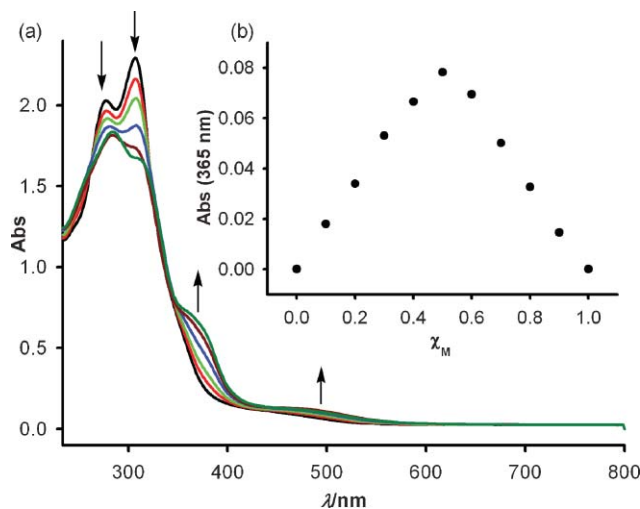


**Fig. 5** (a) Changes in the absorption spectra of **6b** (black) ( $5 \times 10^{-5} \text{ M}$ ) in  $\text{CH}_3\text{CN}$  upon addition of increasing amounts of  $\text{Hg}^{2+}$  metal cation, until 1 equivalent was added (deep green); (b) Job's plot for **6b** and  $\text{Hg}^{2+}$ , indicating the formation of 1 : 1 complexes. The total  $[\mathbf{6b}] + [\text{Pb}^{2+}] = 10^{-4} \text{ M}$ .

The stoichiometry of the complex has also been confirmed by ESI-MS, where peaks at  $m/z$  714 for  $[\mathbf{6a}\text{-Pb}^{2+}]$  complex and at  $m/z$  710 for  $[\mathbf{6b}\text{-Hg}^{2+}]$  complex are observed. Their relative abundance of the isotopic clusters was in good agreement with the simulated spectra of the complex (Fig. 6).

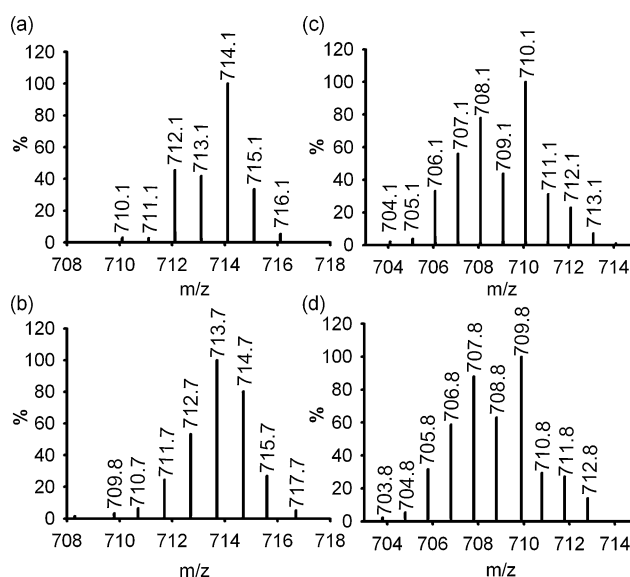


**Fig. 6** Relative abundance of the isotopic cluster for  $[\mathbf{6a}\text{-Pb}^{2+}]$ : (a) simulated; (b) experimental. Relative abundance of the isotopic cluster for  $[\mathbf{6b}\text{-Hg}^{2+}]$ : (c) simulated; (d) experimental.

On the other hand, absorption spectra of receptors **6** in the presence of  $\text{Bu}_4\text{NOH}$  displayed the same changes than those observed with  $\text{HP}_2\text{O}_7^{3-}$  and  $\text{F}^-$  anions. When the spectral evolution of receptors **6** with these anions were performed in the presence of 20 equivalents of acetic acid, the spectral course of the addition matched with that expected for a deprotonation process.

Assessment of the cation affinity also came from observing the extent to which the fluorescence intensity of receptors **6** were affected in the presence of the selected cations. Receptor **6a** exhibits a very weak fluorescence in  $\text{CH}_3\text{CN}$  ( $c = 1 \times 10^{-5}$ ) when excited at  $\lambda_{\text{exc}} = 330$  nm. The emission spectrum shows a structureless band at 484 nm, with rather low quantum yield ( $\Phi = 3.6 \times 10^{-4}$ ).<sup>36</sup> This receptor did not undergo any considerable change in its emission spectrum, upon addition of  $\text{Zn}^{2+}$ ,  $\text{Cd}^{2+}$ , and  $\text{Hg}^{2+}$ . However, in the presence of  $\text{Pb}^{2+}$  metal cations the emission band underwent a red-shift at 515 nm ( $\Delta\lambda = 31$  nm) along with an important chelation-enhanced fluorescence factor (CHEF = 276)<sup>37</sup> and the quantum yield ( $\Phi = 2.2 \times 10^{-2}$ ) resulted in a 61-fold increase compared to that of the receptor **6a** (Fig. 7). The stoichiometry of the complex was also confirmed by the changes in the fluorogenic response of **6a** in the presence of varying concentrations of  $\text{Pb}^{2+}$ , the results indicating the formation of a 1:1 complex with a association constant  $K_a = 8.29 \times 10^5 (\pm 1.39) \text{ M}^{-1}$ .

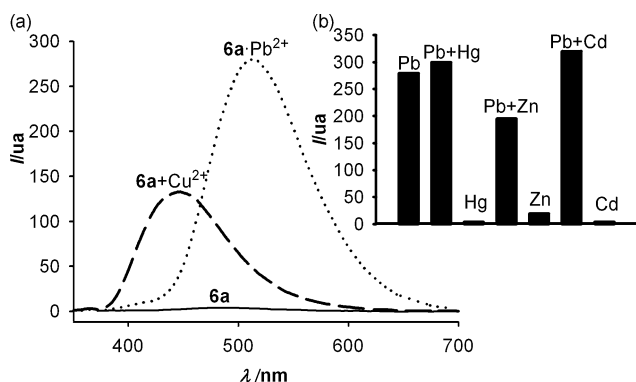


**Fig. 7** (a) Changes in the fluorescence spectra of **6a** ( $1 \times 10^{-5}$  M) in  $\text{CH}_3\text{CN}$  upon addition of  $\text{Pb}^{2+}$  (dotted line) and  $\text{Cu}^{2+}$  (dashed line) metal cations ( $\lambda_{\text{exc}} = 330$  nm). (b) Fluorescence emission intensity of **6a** upon addition of 0.5 equivalents of  $\text{Pb}^{2+}$  in the presence of 0.5 equivalents of interference metal ions in  $\text{CH}_3\text{CN}$ .

The detection limit, calculated as three times the standard deviation of the background noise,<sup>38</sup> was found to be  $5.25 \times 10^{-6}$  M. Remarkably, addition of  $\text{Cu}^{2+}$  metal cations also induced, albeit in a lower extension, a red shift of the emission band by 37 nm and a CHEF = 129 (Fig. 7). Such interesting result may be explained by quenching of the fluorescence of the heterocyclic ring system subunit in the neutral receptor **6a** by the ferrocene unit. Thus, only a weak emission band is observed. Quenching by the ferrocene subunit may occur *via* either electron transfer or energy transfer from the ferrocenyl group that act as an electron-donor, to the excited state of the heterocyclic ring system, acting as an electron-acceptor unit. After oxidation of the neutral receptor **6a** by the  $\text{Cu}^{2+}$  metal cation, as evidenced the above mentioned LSV studies, the electron-donating ability of the ferrocene subunit is reduced and, as a result, the electron transfer is arrested leading to a fluorescence enhancement.<sup>39</sup>

Receptor **6b** also exhibits a very weak fluorescence in  $\text{CH}_3\text{CN}$ , the excitation spectrum revealing  $\lambda_{\text{exc}} = 310$  nm as an ideal excitation wavelength. The emission spectrum shows a weak and structureless band at 507 nm, with a rather low quantum yield ( $\Phi = 6.1 \times 10^{-4}$ ). Fluorescence titration experiments by using the same set of metal cations, demonstrate that only  $\text{Hg}^{2+}$  progressively yielded an important enhancement of the emission band (CHEF = 227) along with a red-shift of the band ( $\Delta\lambda = 28$  nm) and the quantum yield ( $\Phi = 1.9 \times 10^{-2}$ ) resulted in a 31-fold increase compared to that of the receptor **6b** (Fig. 8). From the titration data the stoichiometry of the complex was found to be 1:1, with the association constant  $K_a = 1.07 \times 10^6 (\pm 1.93) \text{ M}^{-1}$  and detection limit  $1.81 \times 10^{-6}$  M. In this case, addition of  $\text{Cu}^{2+}$  metal cations induced extension a blue shift of the emission band by 49 nm and a CHEF = 176.

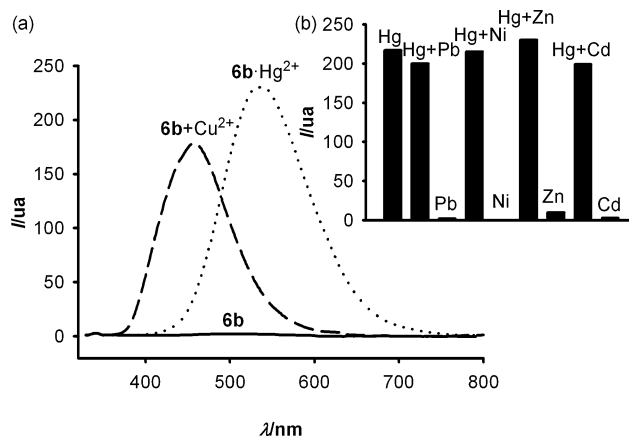


**Fig. 8** (a) Changes in the fluorescence spectra of **6b** ( $1 \times 10^{-5}$  M) in  $\text{CH}_3\text{CN}$  upon addition of  $\text{Hg}^{2+}$  (dotted line) and  $\text{Cu}^{2+}$  (dashed line) metal cations ( $\lambda_{\text{exc}} = 310$  nm). (b) Fluorescence emission intensity of **6b** upon addition of 0.5 equivalents of  $\text{Hg}^{2+}$  in the presence of 0.5 equivalents of interference metal ions in  $\text{CH}_3\text{CN}$ .

Competitive experiments were also carried out by adding  $\text{Pb}^{2+}$  or  $\text{Hg}^{2+}$  (0.5 equivalents) to the solution of **6a** or **6b**, respectively, in the presence of other metal cations (Fig. 7(b) and 8(b)).

For the reported constant to be taken with confidence, we have proved the reversibility of the complexation process by carrying out the following experimental test: 1 equivalent of  $\text{Pb}(\text{ClO}_4)_2$  was added to a solution of the receptor **6a** in  $\text{CH}_2\text{Cl}_2$  to obtain the complex **[6a-Pb<sup>2+</sup>]**, whose UV-vis spectra and  $^1\text{H}$  NMR were recorded. The  $\text{CH}_2\text{Cl}_2$  solution of the complex was washed several times with water. The organic layer was dried, and the optical spectrum, and  $^1\text{H}$  NMR spectrum were recorded and they were found to be the same than that of the free receptor **6a**. Afterwards, 1 equivalent of  $\text{Pb}(\text{ClO}_4)_2$  was added to this solution, and the initial UV-vis and  $^1\text{H}$  NMR spectra of the complex **[6a-Pb<sup>2+</sup>]** were fully recovered. This experiment was carried out over several cycles, and the optical spectrum was recorded after each step, thus demonstrating the high degree of the reversibility of the complexation/decomplexation process. Similar studies were carried out using the receptor **6b** and  $\text{Hg}^{2+}$  metal cation, which confirm the reversibility of this process between this receptor and such cationic metal species (see ESI†).

To support the results obtained by electrochemical and spectroscopic (absorption and emission) experiments, and to obtain

additional information about the coordination mode of these metal cations by receptors **6**, we also performed a  $^1\text{H}$  NMR spectroscopic analysis in  $\text{CD}_3\text{CN}$  solution. The most significant features observed in the  $^1\text{H}$  NMR of both free ligands, **6a** and **6b**, are the following: (i) a singlet ( $\delta = 4.17$  ppm) and two broad singlets ( $\delta = 4.53$  and  $\delta = 5.14$  ppm), corresponding to the three different set of protons existing in the unsubstituted and monosubstituted cyclopentadienyl moieties present in the ferrocene unit; (ii) two doublets associated to the H4 and H5 protons present in both derivatives, which appear at  $\delta = 7.89$  and  $\delta = 8.06$  ppm, in the case of **6a**, and at  $\delta = 8.11$  and  $\delta = 8.21$  ppm, in the case of **6b**; (iii) the signals corresponding to the aromatic and heteroaromatic substituents linked to the 7 and 8 positions of both heterocyclic systems. Interestingly, a common feature observed in the complexation processes is the appearance of a significant downfield shift of the  $^1\text{H}$  NMR signals corresponding to the H4 ( $\Delta\delta = +0.22$  ppm for **6a** and  $\Delta\delta = +0.24$  ppm for **6b**) and H5 ( $\Delta\delta = +0.15$  ppm for **6a** and  $\Delta\delta = +0.38$  for **6b** ppm) protons (see ESI $^\dagger$ ). However, apart from this analogous behaviour, the formation of the complexed species is also accompanied by remarkable differences when their  $^1\text{H}$  NMR spectra are compared. Thus, addition of  $\text{Pb}^{2+}$  to ligand **6a** also promotes a downfield shifting of the ferrocene signals, which peak shapes were progressively broadened as the number of equivalents of the metal cation is increased; however, the phenyl protons remained essentially unaffected during the complexation process (Fig. 9). Although addition of  $\text{Hg}^{2+}$  to ligand **6b** is also accompanied by a downfield shift of all the  $^1\text{H}$  NMR signals corresponding to the ferrocene unit, the two broad singlets due to the two sets of the ferrocene equivalent protons ( $\text{H}_\alpha$  and  $\text{H}_\beta$ ) within the free ligand are now clearly split into four different chemical shift non-equivalent signals attributable to the  $\text{H}_\alpha$ ,  $\text{H}_\alpha'$ ,  $\text{H}_\beta$  and  $\text{H}_\beta'$  present in such monosubstituted cyclopentadienyl ring. On the other hand, as the progressive addition of  $\text{Hg}^{2+}$  to ligand **6b** is taking place two very well defined sets of sharp signals (two doublets and two triple doublets in the  $\delta$  range from 6.7 to 7.8 ppm and from 7.8 to 9.2 ppm, respectively), associated to the protons present within two different pyridine rings are also observed (Fig. 10). This fact clearly indicates a chemical shift non-equivalence of the protons associated to both pyridyl substituents linked to the 7 and 8 position of the heteroaromatic ring.

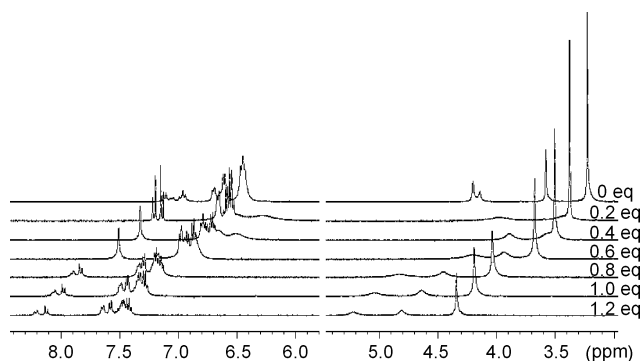


**Fig. 9** Evolution of the  $^1\text{H}$  NMR spectra of **6a** (top), in acetonitrile- $d_3$ , upon addition of aliquots of  $\text{Pb}^{2+}$  until 1.2 equivalents were reached (bottom).

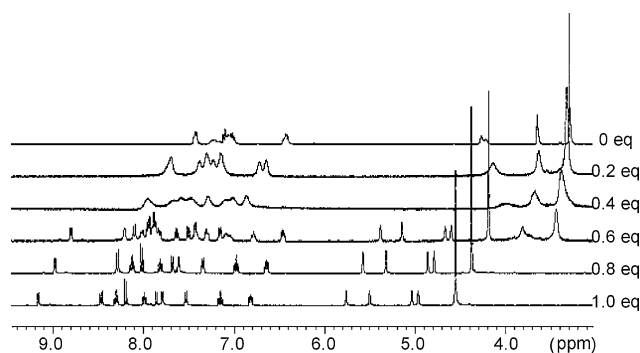


**Fig. 10** Evolution of the  $^1\text{H}$  NMR spectra of **6b** (top), in acetonitrile- $d_3$ , upon addition of aliquots of  $\text{Hg}^{2+}$  until 1 equivalent was reached (bottom).

The above metal ion-induced chemical shift changes support that both metal cations are bound to the imidazole (N1) and quinoxaline (N9) units of the imidazo-quinazoline framework. Additionally, in the case of ligand **6b** the N atom present in the 8-pyridyl substituent is acting in a synergistic way during the complexation process of the  $\text{Hg}^{2+}$  metal cation.

## Conclusions

The synthesis, electrochemical, optical and cation sensing properties of ferrocene-imidazo[4,5-f]quinoxalines **6**, are presented. The synthetic methodology for the preparation of the target molecules involved initial condensation of the appropriate 1,2-dicarbonyl compound with 4-nitro-*o*-phenylenediamine, followed by amination with 4-amino-1,2,4-triazole, reduction of the nitro group of the resulting quinoxaline and finally imidazole-ring formation by condensation with ferrocenecarboxaldehyde under oxidative conditions. Dyad **6a** behaves as a highly selective redox, chromogenic and fluorescent chemosensor molecule for  $\text{Pb}^{2+}$  cations in  $\text{CH}_3\text{CN}$  solutions. Upon complexation with this metal cation the oxidation redox peak is anodically shifted ( $\Delta E_{1/2} = 110$  mV), a new low-energy band appeared at 463 nm, in its UV-vis spectrum, and the emission band is red-shift ( $\Delta\lambda = 31$  nm) along with an important chelation-enhanced fluorescence factor (CHEF = 276). On the other hand, dyad **6b**, bearing two additional pyridine rings as substituents, has shown its ability for sensing  $\text{Hg}^{2+}$  cations: the oxidation peak is anodically higher shifted ( $\Delta E_{1/2} = 300$  mV), a new low-energy band in the absorption spectrum appeared at 483 nm and the emission band was also red-shifted ( $\Delta\lambda = 28$  nm) and underwent an important chelation-enhanced fluorescent factor (CHEF = 227). These changes in the absorption and emission spectra of receptors **6** are accompanied by colour changes, allowing the potential “naked eye” detection of these metal cations (Fig. 11). Linear sweep voltammetry revealed that  $\text{Cu}^{2+}$  cations induced oxidation of the ferrocene unit in both dyads, which is accompanied by an important increase of the emission band. Electrochemical studies on the behaviour of receptors **6** towards anions showed that  $\text{F}^-$  anion induced a strong cathodic shift of the corresponding oxidation waves ( $\Delta E_{1/2} = -300$  mV for **6a** and  $\Delta E_{1/2} = -270$  mV for **6b**), clearly due to a deprotonation process. Whereas, addition of  $\text{HP}_2\text{O}_7^{3-}$  in the presence of acetic acid induced the appearance of a new oxidation wave ( $\Delta E_{1/2} = -80$  mV for **6a** and  $\Delta E_{1/2} = -90$  mV for **6b**), assigned to a recognition process.

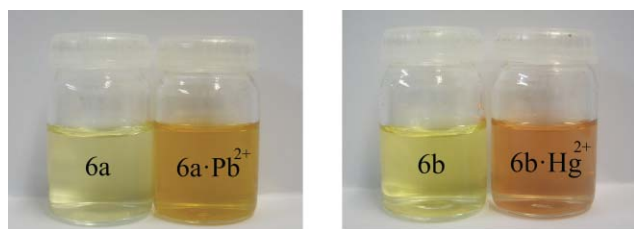


**Fig. 11** Visual features observed in the  $\text{CH}_3\text{CN}$  solutions of  $\text{CH}_3\text{CN}$  solutions of **6a** after addition of  $\text{Pb}^{2+}$  (left), and **6b** after addition of  $\text{Hg}^{2+}$ .

## Experimental

### General

Melting points were determined on a Kofler hot-plate melting point apparatus and are uncorrected.  $^1\text{H}$  and  $^{13}\text{C}$  spectra were recorded on a Bruker AC300, and 400. The following abbreviations for stating the multiplicity of the signals have been used: s (singlet), bs (broad singlet), d (doublet), dd (double of doublets), ddd (double of doublet of doublets), dt (double of triplets), st (pseudotriplet), td (triple of doublets) and q (quaternary carbon). Chemical shifts refer to signals of tetramethylsilane in the case of  $^1\text{H}$  and  $^{13}\text{C}$  spectra. The electron impact (EI) and electrospray (ESI) mass spectra were recorded on a Fisons AUTOSPEC 500 VG spectrometer. Microanalyses were performed on a Carlo Erba 1108 instrument. CV and OSWV techniques were performed with a conventional three-electrode configuration consisting of platinum working and auxiliary electrodes and a  $\text{Ag}/\text{AgCl}$  reference electrode. The experiments were carried out with a  $10^{-3}$  M solution of sample in  $\text{CH}_3\text{CN}$  containing 0.1 M  $(n\text{-C}_4\text{H}_9)_4\text{ClO}_4$  (TBAP) (WARNING: potential formation of highly explosive perchlorate salts or organic derivatives) as supporting electrolyte. All the potential values reported are relative to the decamethylferrocene (DMFc) couple at room temperature. Deoxygenation of the solutions was achieved by bubbling nitrogen for at least 10 min and the working electrode was cleaned after each run. The cyclic voltammograms were recorded with a scan rate increasing from 0.05 to 1.00  $\text{Vs}^{-1}$ , while the OSWV were recorded at a scan rate of 100  $\text{mVs}^{-1}$  with a pulse height of 10 mV and a step time of 50 ms. Typically, receptor ( $1 \times 10^{-3}$  M) was dissolved in  $\text{CH}_3\text{CN}$  (5 mL) and TBAP (base electrolyte) (0.170 g) added. The guest under investigation was then added as a 0.1 M solution in appropriate solvent using a microsyringe whilst the cyclic voltammetric properties of the solution were monitored. DMFc was used as an external reference both for potential calibration and for reversibility criteria. Under similar conditions the DMFc has  $E = -0.07$  V vs. SCE and the anodic peak-cathodic peak separation is 67 mV.

Compounds **3a**,<sup>40</sup> **3b**,<sup>41</sup> **4a**<sup>42</sup> and **5a**<sup>42</sup> were prepared according to the already described procedures.

**Preparation of 5-amino-6-nitro-2,3-di(2-pyridyl)quinoxaline, 4b.** A solution of potassium *t*-butoxide (0.56 g, 5 mmol) in DMSO (10 mL) was added dropwise to a solution of 6-nitro-2,3-di(2-pyridyl)quinoxaline, **3b**, (0.5 g, 1.5 mmol) and 4-amino-1,2,4-triazole (0.84 g, 10 mmol) in DMSO (10 mL). The reaction mixture was stirred at room temperature for 20 min and then poured into a saturated aqueous solution of  $\text{NH}_4\text{Cl}$  (70 mL). The precipitate formed was filtered, washed with *n*-hexane and crystallized from

$\text{EtOH-n-hexane}$  (1 : 1) to give **4b** in 71% yield (0.37 g). Mp: 218–220 °C. Found: C, 62.98; H, 3.29; N, 24.12.  $\text{C}_{18}\text{H}_{12}\text{N}_6\text{O}_2$  requires C, 62.79; H, 3.51; N, 24.41%.  $\delta_{\text{H}}$  (400 MHz;  $\text{CDCl}_3$ ;  $\text{Me}_4\text{Si}$ ) 7.24 (1H, dd,  $J$  4.8 and 0.8 Hz), 7.26 (1H, dd,  $J$  4.8 and 0.8 Hz), 7.31 (1H, d,  $J$  9.6 Hz), 7.80 (1H, td,  $J$  7.6 and 1.6 Hz), 7.81 (1H, td,  $J$  7.6 and 1.6 Hz), 7.91 (1H, d, 7.6 Hz), 7.97 (1H, d, 7.6 Hz), 8.33 (1H, d,  $J$  4.8 Hz), 8.38 (1H, d,  $J$  9.6 Hz);  $\delta_{\text{C}}$  (100 MHz;  $\text{CDCl}_3$ ;  $\text{Me}_4\text{Si}$ ) 115.2 (CH), 123.2 (CH), 123.5 (CH), 124.1 (CH), 124.3 (CH), 126.8 (CH), 127.6 (q), 132.1 (q), 136.7 (CH), 136.8 (CH), 144.2 (q), 144.3 (q), 148.5 (CH), 148.6 (CH), 150.1 (q), 155.4 (q), 156.4 (q), 156.5 (q);  $m/z$  (EI) 344 ( $\text{M}^+$ , 100), 297 (93), 270 (23), 148 (23), 135 (16), 78 (38).

### Preparation of 5,6-diamino-2,3-di(2-pyridyl)quinoxaline, 5b.

To a solution of 5-amino-6-nitro-2,3-di(pyridyl)quinoxaline, **4b**, (0.5 g, 1.45 mmol) in ethanol (40 mL), heated at 50 °C, C/Pd (0.001 g) and hydrazine hydrate (0.5 mL, 10.15 mmol) were added. After the addition of hydrazine was completed, another portion of C/Pd catalyst (0.001 g) was added and the resulted mixture was refluxed for 3 h. On cooling, the suspension obtained was filtered over a Celite pad and the solvent evaporated to dryness under reduced pressure. The resulting red solid obtained was scratched with *n*-pentane, filtered and crystallized from  $\text{EtOH-n-hexane}$  (1 : 1) to give **5b** in 93% yield (0.42 g). Mp: 112–113 °C. Found: C, 68.50; H, 4.21; N, 26.96.  $\text{C}_{18}\text{H}_{14}\text{N}_6$  requires C, 68.78; H, 4.49; N, 26.74%.  $\delta_{\text{H}}$  (400 MHz;  $\text{CDCl}_3$ ;  $\text{Me}_4\text{Si}$ ) 7.20 (1H, ddd,  $J$  7.6, 4.8 and 1.28 Hz), 7.23 (1H, ddd,  $J$  7.6, 4.8 and 1.28 Hz), 7.28 (1H, d,  $J$  8.8 Hz), 7.59 (1H, d,  $J$  8.8 Hz), 7.78 (1H, td,  $J$  7.6 and 2.0 Hz), 7.81 (1H, td,  $J$  7.6 and 1.6 Hz), 7.89 (1H, dt, 7.6 and 0.8 Hz), 7.98 (1H, dt, 7.6 and 0.8 Hz), 8.36 (1H, m);  $\delta_{\text{C}}$  (100 MHz;  $\text{CDCl}_3$ ;  $\text{Me}_4\text{Si}$ ) 119.2 (CH), 122.1 (CH), 122.4 (CH), 122.5 (CH), 123.7 (CH), 123.9 (CH), 127.1 (q), 132.0 (q), 133.2 (q), 136.0 (CH), 136.1 (CH), 136.2 (CH), 147.9 (CH), 148.1 (CH), 148.6 (q), 149.5 (q), 157.5 (q), 157.6 (q);  $m/z$  (EI) 314 ( $\text{M}^+$ , 100), 296 (26), 286 (41), 236 (11), 156 (26), 142 (18), 105 (24), 78 (40).

**General procedure for the preparation of 2-ferrocenyl-7,8-disubstituted-3H-imidazo[4,5-f]quinoxalines, 6.** To a solution of the appropriate 5,6-diaminoquinoxaline **5** (4.37 mmol) in nitrobenzene (10 mL) ferrocenecarboxaldehyde (0.94 g, 4.37 mmol) was added. Then, 0.5 mL of acetic acid was added and the reaction mixture was stirred for 15 h at 70 °C. Afterwards, an aqueous solution of  $\text{NaHCO}_3$  was added until pH = 7 was achieved. Then, the resulting mixture was poured into water (50 mL) and extracted with  $\text{CHCl}_3$  (2  $\times$  50 mL). The organic phase was dried over anhydrous  $\text{MgSO}_4$ , filtered and concentrated under vacuum to give a residue which was purified by column chromatography by using dichloromethane-*n*-hexane-methanol (9 : 1 : 0.25) or dichloromethane-methanol (9 : 1) as eluent to give compounds **6a** and **6b**, respectively.

**2-Ferrocenyl-7,8-diphenyl-3H-imidazo[4,5-f]quinoxalines, 6a.** 48% yield (1.06 g). Mp: 201–203 °C. Found: C, 73.71; H, 4.60; N, 11.29.  $\text{C}_{31}\text{H}_{22}\text{FeN}_4$  requires C, 73.53; H, 4.38; N, 11.06%.  $\delta_{\text{H}}$  (400 MHz; MeOD;  $\text{Me}_4\text{Si}$ ) 4.17 (5H, s), 4.49 (2H, st), 5.16 (2H, st), 7.35 (1H, m), 7.45 (1H, m), 7.47 (1H, dd,  $J$  6.4 and 2.0 Hz), 7.55 (1H, dd,  $J$  6.4 and 1.2 Hz), 7.89 (1H, d,  $J$  9.2 Hz), 7.98 (1H, d,  $J$  9.2 Hz);  $\delta_{\text{H}}$  (400 MHz;  $\text{CD}_3\text{CN}$ ;  $\text{Me}_4\text{Si}$ ) 4.17 (5H, s), 4.52 (2H, bs), 5.14 (2H, bs), 7.40 (6H, m), 7.55 (3H, dd,  $J$  6.4 and 1.6 Hz), 7.64 (1H, d,  $J$  6.4), 7.89 (1H, d,  $J$  8.8 Hz), 8.06 (1H, d,

J 8.8 Hz);  $\delta_{\text{C}}$  (100 MHz; MeOD; Me<sub>4</sub>Si) 68.8 (CH), 70.8 (CH), 71.6 (CH), 73.9 (q), 124.0 (CH), 129.1 (CH), 129.3 (CH), 129.7 (CH), 129.8 (CH), 131.1 (CH), 131.2 (CH), 131.3 (q), 131.5 (q), 139.6 (q), 140.5 (q), 140.6 (q), 152.4 (q), 153.6 (q), 156.4 (q);  $m/z$  (ESI) 507 ( $M^+$ +1, 100).

**2-Ferrocenyl-7,8-di-(2-pyridyl)-3H-imidazo[4,5-f]quinoxalines, 6b.** 43% yield (0.95 g). Mp: 197–199 °C. Found: C, 68.23; H, 3.81; N, 16.77. C<sub>29</sub>H<sub>20</sub>FeN<sub>6</sub> requires C, 68.52; H, 3.97; N, 16.53%.  $\delta_{\text{H}}$  (400 MHz; CDCl<sub>3</sub>; Me<sub>4</sub>Si) 4.10 (5H, s), 4.36 (2H, st), 4.99 (2H, st), 7.21 (1H, m), 7.51 (1H, t,  $J$  7.2 Hz), 7.60 (1H, t,  $J$  7.2 Hz), 7.75 (1H, td,  $J$  8.0 and 1.2 Hz), 7.92 (1H, d,  $J$  8.0 Hz), 7.95 (1H, d,  $J$  8.8 Hz), 8.14 (1H, d,  $J$  8.8 Hz), 8.41 (1H, d,  $J$  4.0 Hz), 8.51 (1H, d,  $J$  4.4 Hz);  $\delta_{\text{H}}$  (400 MHz; CD<sub>3</sub>CN); Me<sub>4</sub>Si) 4.18 (5H, s), 4.53 (2H, bs), 5.13 (2H, bs), 7.32 (2H, dd,  $J$  7.2 and 1.8 Hz), 7.94 (3H, m), 7.95 (1H, d,  $J$  9.0), 8.07 (1H, m); 8.08 (1H, d,  $J$  9.0 Hz), 8.32 (2H, m);  $\delta_{\text{C}}$  (100 MHz; CDCl<sub>3</sub>; Me<sub>4</sub>Si) 67.0 (CH), 69.4 (CH), 69.8 (CH), 72.9 (q), 122.4 (CH), 123.0 (CH), 123.9 (CH), 124.1 (CH), 135.8 (CH), 136.2 (CH), 138.4 (q), 148.1 (CH), 149.2 (q), 149.8 (q), 154.3 (q), 157.0 (q);  $m/z$  (EI) 508 ( $M^+$ , 100), 442 (13), 430 (12), 254 (11).

## Acknowledgements

We gratefully acknowledge the financial support from MICINN-Spain, Project CTQ2008-01402 and Fundación Séneca (Agencia de Ciencia y Tecnología de la Región de Murcia) project 04509/GERM/06 (Programa de Ayudas a Grupos de Excelencia de la Región de Murcia, Plan Regional de Ciencia y Tecnología 2007/2010).

## Notes and references

- (a) *Fluorescent Chemosensors for Ion and Molecule Recognition*, ed. A. W. Czarnik, American Chemical Society, Washington, DC, 1993; (b) A. P. de Silva, H. Q. N. Gunaratne, T. Gunnlaugsson, A. J. M. Huxley, C. P. McCoy, J. T. Rademacher and T. E. Rice, *Chem. Rev.*, 1997, **97**, 1515–1566.
- J. M. Benoit, W. F. Fitzgerald and A. W. Damman, *Environ. Res.*, 1998, **78**, 118–133.
- A. Renzoni, F. Zino and E. Franchi, *Environ. Res.*, 1998, **77**, 68–72.
- O. Malm, *Environ. Res.*, 1998, **77**, 73–78.
- Mercury Update: Impact on Fish Advisories*. EPA Fact Sheet EPA-823-F-01-011; EPA. Office, of Water, Washington, DC, 2001.
- (a) P. Grandjean, P. Weihe, R. F. White and F. Debes, *Environ. Res.*, 1998, **77**, 165–172; (b) D. W. Boening, *Chemosphere*, 2000, **40**, 1335–1351; (c) H. H. Harris, I. J. Pickering and G. N. George, *Science*, 2003, **301**, 1203–1203.
- (a) X. B. Feng, P. Li, G. L. Qiu, S. Wang, G. H. Li, L. H. Shang, B. Meng, H. M. Jiang, W. Y. Bai, Z. G. Li and X. W. Fu, *Environ. Sci. Technol.*, 2008, **42**, 326–332; (b) E. M. Krupp, A. Mestrot, J. Wielgus, A. A. Meharg and J. Feldmann, *Chem. Commun.*, 2009, 4257–4259.
- (a) E. M. Nolan and S. J. Lippard, *Chem. Rev.*, 2008, **108**, 3443–3480; (b) P. Molina, A. Tárraga and A. Caballero, *Eur. J. Inorg. Chem.*, 2008, 4301–4317.
- (a) O. Brummer, J. J. La Clair and K. D. Janda, *Org. Lett.*, 1999, **1**, 415–418; (b) M. J. Choi, M. Y. Kim and S. K. Chang, *Chem. Commun.*, 2001, 1664–1665; (c) Y. Zhao and Z. Q. Zhong, *Org. Lett.*, 2006, **8**, 4715–4717; (d) S. Tatay, P. Gaviña, E. Coronado and E. Palomares, *Org. Lett.*, 2006, **8**, 3857–3860; (e) Y. Zhao and Z. Q. Zhong, *J. Am. Chem. Soc.*, 2006, **128**, 9988–9989; (f) M. K. Nazeeruddin, D. Di Censo, R. Humphry-Baker and M. Grätzel, *Adv. Funct. Mater.*, 2006, **16**, 189–194; (g) E. Coronado, J. R. Galán-Mascarós, C. Martí-Gastaldo, E. Palomares, J. R. Durrant, R. Vilar, M. Grätzel and M. K. Nazeeruddin, *J. Am. Chem. Soc.*, 2005, **127**, 12351–12356; (h) T. Balaji, S. A. El-Safty, H. Matsunaga, T. Hanaoka and F. Mizukami, *Angew. Chem., Int. Ed.*, 2006, **45**, 7202–7208; (i) S. Y. Lin, S. M. Wu and C. H. Chen, *Angew. Chem., Int. Ed.*, 2006, **45**, 4948–4951; (j) C. Diez-Gil, A. Caballero, I. Ratera, A. Tárraga, P. Molina and J. Veciana, *Sensors*, 2007, **7**, 3481–3488.
- (a) D. Jiménez, R. Martínez-Máñez, F. Sancenón and J. Soto, *Tetrahedron Lett.*, 2004, **45**, 1257–1259; (b) A. Caballero, V. Lloveras, D. Curiel, A. Tárraga, A. Espinosa, R. García, J. Vidal-Gancedo, C. Rovira, K. Wurst, P. Molina and J. Veciana, *Inorg. Chem.*, 2007, **46**, 825–838.
- (a) A. Caballero, R. Martínez, V. Lloveras, I. Ratera, J. Vidal-Gancedo, K. Wurst, A. Tárraga, P. Molina and J. Veciana, *J. Am. Chem. Soc.*, 2005, **127**, 15666–15667; (b) E. M. Nolan and S. J. Lippard, *J. Am. Chem. Soc.*, 2003, **125**, 14270–14271; (c) J. V. Ros-Lis, M. D. Marcos, R. Martínez-Máñez, K. Rurack and J. Soto, *Angew. Chem., Int. Ed.*, 2005, **44**, 4405–4407; (d) I. B. Kim and U. H. F. Bunz, *J. Am. Chem. Soc.*, 2006, **128**, 2818–2819; (e) I. B. Kim, B. Erdogan, J. N. Wilson and U. H. F. Bunz, *Chem.–Eur. J.*, 2004, **10**, 6247–6254; (f) S. J. Ou, Z. H. Lin, C. Y. Duan, H. T. Zhang and Z. P. Bai, *Chem. Commun.*, 2006, 4392–4394; (g) J. B. Wang and H. Qian, *Org. Lett.*, 2006, **8**, 3721–3724; (h) R. Martínez, F. Zapata, A. Caballero, A. Espinosa, A. Tárraga and P. Molina, *Org. Lett.*, 2006, **8**, 3235–3238; (i) A. Ono and H. Togashi, *Angew. Chem., Int. Ed.*, 2004, **43**, 4300–4302; (j) S. Yoon, A. E. Albers, A. P. Wong and C. J. Chang, *J. Am. Chem. Soc.*, 2005, **127**, 16030–16031; (k) X. J. Zhu, S. T. Fu, W. K. Wong, H. P. Guo and W. Y. Wong, *Angew. Chem., Int. Ed.*, 2006, **45**, 3150–3154; (l) C. Diez-Gil, R. Martínez, I. Ratera, A. Tárraga, P. Molina and J. Veciana, *J. Mater. Chem.*, 2008, **18**, 1997–2002; (m) M. Yuan, W. Zhou, X. Liu, M. Zhu, J. Li, X. Yin, H. Zheng, Z. Zuo, C. Ouyang, H. Liu, Y. Li and D. Zhu, *J. Org. Chem.*, 2008, **73**, 5008–5014; (n) D. Wu, W. Huang, Z. Lin, C. Duan, C. He, S. Wu and D. Wang, *Inorg. Chem.*, 2008, **47**, 7190–7201; (o) W. Huang, C. Song, C. He, G. Lv, X. Hu, X. Zhu and C. Duan, *Inorg. Chem.*, 2009, **48**, 5061–5072.
- J. S. Lin-Fu, Lead Poisoning: A Century of Discovery and Rediscovery, in *Human Lead Exposure*, ed H. L. Needleman, Lewis Publishing, Boca Raton, FL, 1992.
- A. R. Flegal and D. R. Smith, *Environ. Res.*, 1992, **58**, 125–133.
- E. S. Claudio, H. A. Godwin and J. S. Magyar, *Prog. Inorg. Chem.*, 2003, **51**, 1–144 and references therein.
- World Health Organization, *Guidelines for drinking-water quality*, Geneva, 2nd edn, 1996, vol. 2, p. 940.
- M. R. Hopkins, A. S. Ettinger, M. Hernández-Avila, J. Schwartz, M. M. Tellez-Rojo, H. Lamadrid-Figueroa, D. Bellinger, H. Hu and R. O. Wright, *Environ. Health Perspect.*, 2008, **116**, 1261–1266.
- D. S. McClure, *J. Chem. Phys.*, 1952, **20**, 682–686.
- A. W. Varnes, R. B. Dodson and E. L. Whery, *J. Am. Chem. Soc.*, 1972, **94**, 946–950.
- S. Deo and H. A. Godwin, *J. Am. Chem. Soc.*, 2000, **122**, 174–175.
- (a) P. Chen, B. Greenberg, S. Taghvi, C. Romano, D. van der Lelie and C. He, *Angew. Chem., Int. Ed.*, 2005, **44**, 2715–2719; (b) H. Wang, Y. Kim, H. Liu, Z. Zhu, S. Bamrungsap and W. Tan, *J. Am. Chem. Soc.*, 2009, **131**, 8221–8226; (c) C.-V. Liu, C.-C. Huang and H.-T. Chang, *Anal. Chem.*, 2009, **81**, 2383–2387.
- (a) J. Liu and Y. Lu, *J. Am. Chem. Soc.*, 2000, **122**, 10466–10467; (b) J. Liu and Y. Lu, *J. Am. Chem. Soc.*, 2003, **125**, 6642–6643; (c) J. Liu and Y. Lu, *J. Am. Chem. Soc.*, 2004, **126**, 12298–12305; (d) I. H. Chang, J. J. Tulock, J. Liu, W.-S. Kim, D. M. Cannon Jr., Y. Lu, P. W. Bohn, J. V. Sweedler and D. M. Cropek, *Environ. Sci. Technol.*, 2005, **39**, 3756–376; (e) X. Zhu, Z. Liu, L. Chen, B. Qiu and G. Chen, *Chem. Commun.*, 2009, 6050–6052.
- I.-K. Kim, A. Dunkhorst, J. Gilbert and U. H. F. Bunz, *Macromolecules*, 2005, **38**, 4560–4562.
- (a) J. Y. Kwon, Y. J. Jang, Y. J. Lee, K. M. Kim, M. S. Seo, W. Nam and J. Yoon, *J. Am. Chem. Soc.*, 2005, **127**, 10107–10111; (b) K. Kavallieratos, J. M. Rosenberg, W.-Z. Chen and T. Ren, *J. Am. Chem. Soc.*, 2005, **127**, 6514–6515; (c) J. Y. Lee, S. K. Kim, J. H. Jung and J. S. Kim, *J. Org. Chem.*, 2005, **70**, 1463–1466; (d) J.-M. Liu, J.-H. Bu, Q.-Y. Zheng, C.-F. Chen and Z.-T. Huang, *Tetrahedron Lett.*, 2006, **47**, 1905–1908; (e) R. Metivier, I. Leray and B. Valeur, *Chem. Commun.*, 2003, 996–997; (f) R. Metivier, I. Leray and B. Valeur, *Chem.–Eur. J.*, 2004, **10**, 4480–4490; (g) C.-T. Chen and W.-P. Huang, *J. Am. Chem. Soc.*, 2002, **124**, 6246–6247; (h) L.-J. Ma, Y.-F. Liu and Y. Wu, *Chem. Commun.*, 2006, 2702–2704; (i) F.-Y. Wu, S. W. Bae and J.-I. Hong, *Tetrahedron Lett.*, 2006, **47**, 851–8854; (j) Q. He, E. W. Miller, A. P. Wong and C. J. Chang, *J. Am. Chem. Soc.*, 2006, **128**, 9316–9317; (k) M. Crego-Calama and D. N. Reinhoudt, *Adv. Mater.*, 2001, **13**, 1171–1174; (l) L. Ma, H. Li and Y. Wu, *Sens. Actuators, B*, 2009, **143**, 25–29; (m) L. Marbella, B. Serli-Mitasev and P. Basu, *Angew. Chem., Int. Ed.*, 2009, **48**, 3996–3998;

- (n) E. Roussakis, S. A. Pergantis and H. E. Katerinopoulos, *Chem. Commun.*, 2008, 6221–6223; (o) S. H. Kim, A. Hamdi, Y. H. Lee, J. H. Lee, J. S. Kim and J. Vicens, *J. Inclusion Phenom. Macrocyclic Chem.*, 2010, **66**, 133–137.
- 24 (a) F. Zapata, A. Caballero, A. Espinosa, A. Tárraga and P. Molina, *Org. Lett.*, 2008, **10**, 41–44; (b) F. Zapata, A. Caballero, A. Espinosa, A. Tárraga and P. Molina, *J. Org. Chem.*, 2009, **74**, 4787–4796.
- 25 (a) H. Xue, X.-J. Tang, L.-Z. Wu, L.-P. Zhang and C.-H. Tung, *J. Org. Chem.*, 2005, **70**, 9727–9734; (b) D. Remeter, P. Blanchard, M. Allain, I. Grosu and J. Roncali, *J. Org. Chem.*, 2007, **72**, 5285–5290; (c) A. Caballero, A. Espinosa, A. Tárraga and P. Molina, *J. Org. Chem.*, 2008, **73**, 5489–5497.
- 26 T. Yamamoto, K. Sugiyama, T. Kushida, T. Inoue and T. Kanbara, *J. Am. Chem. Soc.*, 1996, **118**, 3930–3937.
- 27 (a) C. B. Black, B. Andrioletti, A. C. Try, C. R. Ruyper and J. L. Sessler, *J. Am. Chem. Soc.*, 1999, **121**, 10438–10439; (b) P. Anzenbacher Jr., A. C. Try, H. Miyaji, K. Jursíková, V. M. Lynch, M. Marquez and J. L. Sessler, *J. Am. Chem. Soc.*, 2000, **122**, 10268–10272; (c) D. Aldakov and P. Anzenbacher Jr., *Chem. Commun.*, 2003, 1394–1395; (d) S. V. Shevchuk, V. M. Lynch and J. L. Sessler, *Tetrahedron*, 2004, **60**, 11283–11291; (e) T. Ghosh, B. G. Maiya and M. W. Wong, *J. Phys. Chem. A*, 2004, **108**, 11249–11259; (f) T. Wang, Y. Bai, L. Ma and X.-P. Yan, *Org. Biomol. Chem.*, 2008, **6**, 1751–1755.
- 28 F. Zapata, A. Caballero, A. Espinosa, A. Tárraga and P. Molina, *Inorg. Chem.*, 2009, **48**, 11566–11575.
- 29 (a) P. D. Beer, *Chem. Soc. Rev.*, 1989, **18**, 409–450; (b) P. D. Beer, P. A. Gale and G. Z. Chen, *Coord. Chem. Rev.*, 1999, **185–186**, 3–36.
- 30 Specfit/32 Global Analysis System, 1999–2004 Spectrum Software Associates (<http://www.bio-logic.info/specfitsup/index.html>) The Specfit program was acquired from Bio-logic, S.A. in January 2005. The equation to be adjusted by nonlinear regression using the above-mentioned software was  $\Delta A / b = \{K_{11} \Delta \epsilon_{HG} [H]_{tot} [G]\} / \{1 + K_{11} [H]\}$ , where H = host, G = guest, HG = complex,  $\Delta A$  = variation in the absorption,  $b$  = cell width,  $K_{11}$  = association constant for a 1 : 1 model, and  $\Delta \epsilon_{HG}$  = variation of molar absorptivity.
- 31  $Li^+$ ,  $K^+$ ,  $Mg^{2+}$ ,  $Cd^{2+}$ , Ni and  $Pb^{2+}$  were added as perchlorate salts, while  $Na^+$ ,  $Ca^{2+}$ ,  $Cu^{2+}$ ,  $Zn^{2+}$  and  $Hg^{2+}$  were added as triflate salts.
- 32 The criteria applied for reversibility was a separation of 60 mV between cathodic and anodic peaks, a ratio for the intensities of the cathodic and anodic currents  $I_c/I_a$  of 1.0, and no shift of the halfwave potentials with varying scan rates.
- 33 (a) S. R. Miller, D. A. Gustowski, Z. H. Chen, G. W. Gokel, L. Echegoyen and A. E. Kaifer, *Anal. Chem.*, 1988, **60**, 2021–2024; (b) J. C. Medina, T. T. Goodnow, M. T. Rojas, J. L. Atwood, A. E. Kaifer and G. K. Gokel, *J. Am. Chem. Soc.*, 1992, **114**, 10583–10595.
- 34 F. Otón, A. Tárraga, A. Espinosa, M. D. Velasco and P. Molina, *Dalton Trans.*, 2006, 3685–3692.
- 35 F. Zapata, A. Caballero, A. Espinosa, A. Tárraga and P. Molina, *J. Org. Chem.*, 2008, **73**, 4034–4044.
- 36 The fluorescence quantum yields were measured with respect to anthracene as standard ( $\Phi = 0.27$ ) (W. R. Dawson, and M. W. Windsor, *J. Phys. Chem.* 1968, **72**, 3251–3260) using the equation  $\Phi_x / \Phi_s = (S_x / S_s) [(1 - 10^{-As}) / (1 - 10^{-Ax})]^2 (n_s^2 / n_x^2)$  where x and s indicate the unknown and standard solution, respectively,  $\Phi$  is the quantum yield, S is the area under the emission curve A is the absorbance at the excitation wavelength and n is the index of refraction.
- 37 CHEF is defined as the  $I_{max} / I_o$ , where  $I_{max}$  corresponds to the maximum emission intensity of the receptor-metal complex, while  $I_o$  is the maximum emission intensity of the free receptor.
- 38 M. Shortreed, R. Kopelman, M. Kuhn and B. Hoyland, *Anal. Chem.*, 1996, **68**, 1414–1418.
- 39 (a) R. Martínez, I. Ratera, A. Tárraga, P. Molina and J. Veciana, *Chem. Commun.*, 2006, 3809–3811; (b) F. Zapata, A. Caballero, A. Espinosa, A. Tárraga and P. Molina, *Dalton Trans.*, 2009, 3900–3902.
- 40 J.-F. Zhou, G.-X. Gong, S.-J. Zhi and X.-L. Duan, *Synth. Commun.*, 2009, **39**, 3743–3754.
- 41 A. Kleineweischede and J. Mattay, *Chem. Eur. J.*, 2006, **4**, 947–957.
- 42 F. I. Abdel-Hay and M. Anwar, *Egyptian J. Chem.*, 1993, **25**, 335–342.